

# NORTHERN HEMISPHERE TELECONNECTION INDICES AND THE MASS BALANCE OF SVALBARD GLACIERS

RICHARD WASHINGTON<sup>a,\*</sup>, ANDREW HODSON<sup>b</sup>, ELISABETH ISAKSSON<sup>c</sup> and OLIVER MACDONALD<sup>a</sup>

<sup>a</sup> *School of Geography, University of Oxford, Mansfield Rd, Oxford, OX1 3TB, UK*

<sup>b</sup> *Department of Geography, University of Sheffield, Sheffield, S10 2TN, UK*

<sup>c</sup> *Norsk Polarinstitutt, N-9001 Tromsø, Norway*

*Received 1 September 1998*

*Revised 8 September 1999*

*Accepted 21 September 1999*

## ABSTRACT

Links between modes of objectively defined Northern Hemisphere atmospheric variability and the mass balance indices from two glaciers in Svalbard covering the period 1966/1967–1995 are explored in this paper. Principal components of the mass balance indices have been used to calculate two indices, one representing Summer melt and the other mass balance related to winter snow accumulation. Correlations between the time coefficients of these principal components and a set of Northern Hemisphere modes of atmospheric variability provide insight into the controls associated with glacial mass balance. Summer melt is associated with the East Atlantic Jet Pattern in the Boreal spring, but significant lead correlations with the Tropical Northern Hemisphere pattern and the West Pacific Pattern also occur. The strongest simultaneous correlations with the winter snow accumulation index result from the modulation of the atmospheric circulation by the North Pacific pattern. The strongest precursor to winter snow accumulation occurs through a phase of the well known Pacific North America pattern and Tropical North American pattern which relate to ENSO. It appears that controls of glacial mass balance in Svalbard may be traced, in part, to heat flux exchanges in the tropical Pacific Ocean. The time delay for the signal to reach the high Arctic suggests predictability potential of glacial mass balance parameters. Copyright © 2000 Royal Meteorological Society.

KEY WORDS: Northern Hemisphere teleconnections; Pacific North American; Tropical Northern Hemisphere; El Niño–Southern Oscillation; glaciers; mass balance; Svalbard; Arctic

## 1. INTRODUCTION

That glacial mass balance indicates an important mix of climatic signals has long been recognized (Haeberli, 1995). For this reason, much recent attention has focussed on the mass balance of glaciers (Haeberli and Hoelzle, 1995; Warrick *et al.*, 1996). Analyses of the controls on glacial mass balance often concentrate on small-scale mass and energy budget studies where detailed on-glacier measurements, or glacier behaviour are related to nearby weather variables (e.g. Hastenrath and Kruss, 1988; Ishikawa *et al.*, 1992; Fleming and Dowdeswell, 1997). Fewer studies try to link such energy budget studies with the broader synoptic patterns (e.g. Yarnal, 1984a,b; Hay and Fitzharris, 1988; Fitzharris *et al.*, 1992; Pohjola and Rogers, 1997a,b; Hodson *et al.*, 1998), while investigations of teleconnections or planetary scale links to glacial mass balance (e.g. Mote, 1998) are scarce.

A feature of climatological research undertaken over the last few decades has been the investigation of planetary-wide associations between time series in the atmosphere–cryosphere–ocean system. Links have been shown to exist, for example, between heat fluxes in the tropical Pacific and sea ice extent in both the Arctic and Antarctica (Gloersen, 1995), as well as between sea level pressure variability in the subtropical and mid-latitude Atlantic and temperature and precipitation variability across much of northern Europe (Hurrell, 1995, 1996). Research that has attempted to link glacial mass balance with global climate

\* Correspondence to: School of Geography, University of Oxford, Mansfield Rd, Oxford, OX1 3TB, UK; e-mail: richard.washington@geog.ox.ac.uk

variability has produced some intriguing insights. Lindeman and Oerlemans (1987) show statistical associations between glacier mass balance of 30 glaciers and 500 hPa geopotential height which draws attention to the importance of planetary waves. Links between mass balance characteristics of glaciers in distant regions have similarly been reported. Tyson *et al.* (1997) have provided evidence for teleconnections between glacial advances on the west coast of New Zealand and extended spells of drought years in South Africa, also thought to result from planetary waves in the zonal westerlies.

This paper examines a data set of mass balance indices for two glaciers in Svalbard. Indices derived from this data by means of principal components are correlated with the time series of modes of Northern Hemisphere atmospheric variability at simultaneous, lag and lead times. The purpose of this work is to determine links between the glacial mass balance indices and known modes of atmospheric variability. The modes used derive from an extensive set of research done on the Northern Hemisphere circulation. In the next section (Section 2) we offer a brief description of the glaciers, the local study region and the mass balance data. Details of the Northern Hemisphere teleconnection modes and the indices used to reflect the temporal amplitudes of these modes follow in Section 3. Statistical methods are outlined in Section 4 while Section 5 outlines the derivation of mass balance indices. Correlations between the glacier mass balance parameters and the modes of atmospheric variability are presented in Section 6. Interpretation of these results and conclusions follow in Sections 7 and 8, respectively.

## 2. MASS BALANCE DATA

Two glaciers, namely Midre Lovénbreen and Austre Brøggerbreen, located on the southern shore of Kongsfjorden, northwest Spitsbergen are examined (see Figure 1). Both glaciers are relatively small and lie

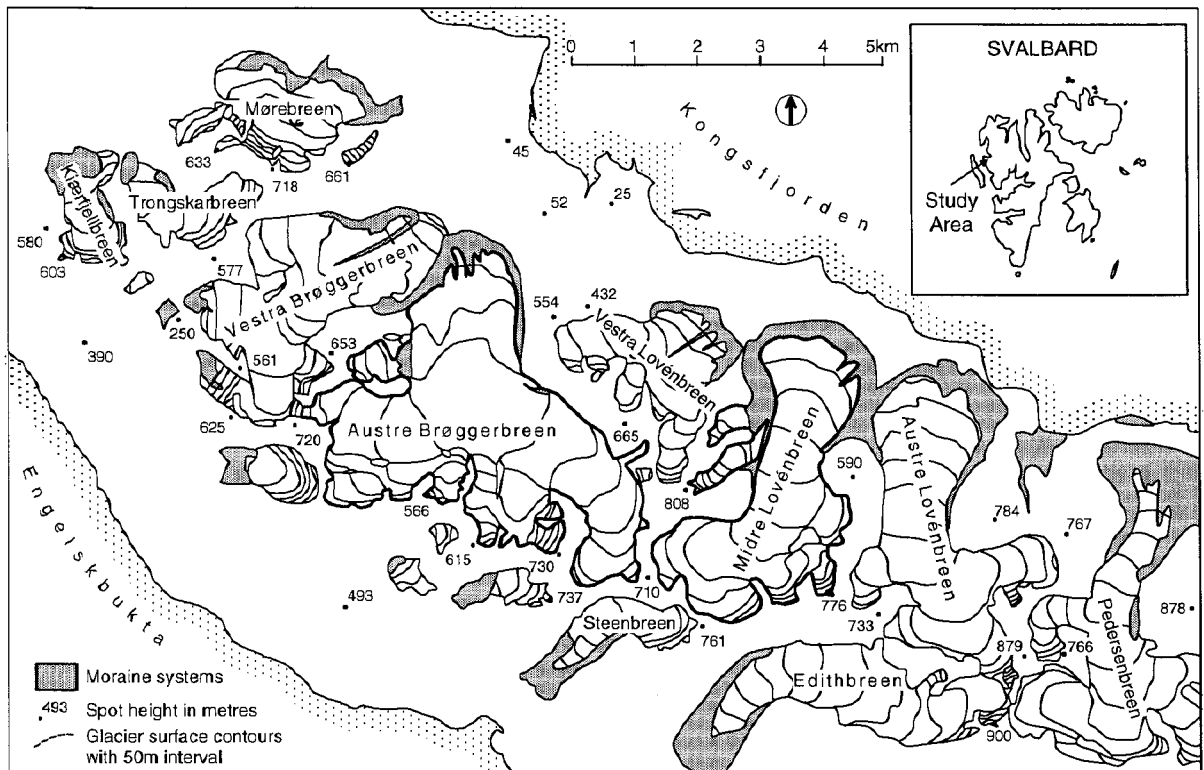


Figure 1. Northwest Spitsbergen showing the locations of Midre Lovénbreen and Austre Brøggerbreen

< 5 km apart on the Brøgger peninsula (Brøggerhalvøya). The mass balance records obtained from the two glaciers constitute the longest and most complete mass balance records available from Svalbard. As a result, the glaciers have received considerable glaciological attention in the past including: the determination of ice volumes from radio echo sounding techniques (e.g. Hagen and Sætrang, 1991), the examination of their hydrological characteristics, particularly those of Austre Brøggerbreen (Repp, 1988; Hodson *et al.*, 1998), and the modelling of their mass balance adjustments to recent climate change (Lefauconnier and Hagen, 1990; Fleming and Dowdeswell, 1997). The two glacier basins span altitudinal ranges from  $\sim 10$ –700 m asl, although Midre Lovénbreen has a much greater proportion of its mass at high elevation than Austre Brøggerbreen. Hence, the mean accumulation area ratios for the two glaciers over the interval 1966–1997 are 36% and 26% for Midre Lovénbreen and Austre Brøggerbreen, respectively.

The data examined here are the summer, winter and net mass balances (hereafter  $B_s$ ,  $B_w$  and  $B_n$ , respectively), together with the following indices derived from the mass balance data: the accumulation area ratio (AAR) and the equilibrium line altitude (ELA). The mass balance estimates were derived for real budget years and further details of the data are reported by Hagen and Liestøl (1990). An analysis of the  $B_n$  data with longer air temperature records by Lefauconnier and Hagen (1990), has shown that both glaciers have experienced a large  $B_n$  deficit since 1918, although slight summer cooling coupled with an increase in winter precipitation has reduced the  $B_n$  deficit since 1969 (see Figure 2). As a consequence, Austre Brøggerbreen and Midre Lovénbreen have experienced net mass losses of 10.4 and 12.7 m (water equivalent), respectively, over the interval 1967–1997.

### 3. NORTHERN HEMISPHERE MODES OF VARIABILITY

The definition of modes of atmospheric variability in the Northern Hemisphere draws on a rich history of research beginning with Walker (1924) and Walker and Bliss (1932). Interest in Northern Hemisphere teleconnections was revived in the late 1970s (e.g. Van Loon and Rogers, 1978; Rogers and Van Loon, 1979), but it was the work of Wallace and Gutzler (1981), Horel (1981), Esbensen (1984) and later that of Mo and Livezey (1986) and Barnston and Livezey (1987) that saw much of the definitive progress. A comprehensive re-analysis of Northern Hemisphere variability patterns has been undertaken by Bell (1998) using newly available 700 hPa height data. An outline of Northern Hemisphere modes of atmospheric variability shown (later) to have statistically significant links with mass balance indices in Svalbard is provided in this section. Atlantic based patterns are considered before those modes resident in the Pacific or North America. This section draws closely on Bell's (1998) definitions.

The North Atlantic Oscillation (NAO) is one of the dominant modes of Northern Hemisphere climate variability (Walker and Bliss, 1932; Van Loon and Rogers, 1978; Wallace and Gutzler, 1981) and is present in all seasons (Barnston and Livezey, 1987). The signature of NAO is a north–south dipole of anomalies, with centres over Greenland/Iceland and the Azores. The positive phase is defined as below normal pressure in the region of the Icelandic low and above normal pressure in the Azores (corresponding with a steepening of the mean geostrophic gradient). This leads to an enhanced Atlantic storm track and anomalously high transport of moisture and heat by transient eddies (Hurrell, 1995), corresponding to changed precipitation and temperature patterns extending from eastern North America to western and central Europe, and into Scandinavia, Siberia and central Russia (Walker and Bliss, 1932; Van Loon and Rogers, 1978; Rogers and Van Loon 1979; Hurrell, 1995). Important seasonal changes to the background climatology include a westward shift to both the Azores high and Icelandic low during the Northern Hemisphere summer while both features locate further to the east during winter.

Atlantic variability in the autumn, winter and spring is also controlled by the East Atlantic (EA) pattern (Barnston and Livezey, 1987). Similar to the NAO, this pattern consists of a north–south dipole but extends across the entire North Atlantic basin with a line of separation through England and France (Barnston and Livezey, 1987). The EA pattern is distinct in that the anomaly centres are concentrated near the nodal lines of the NAO dipole, resembling a southward shifted NAO, so that the

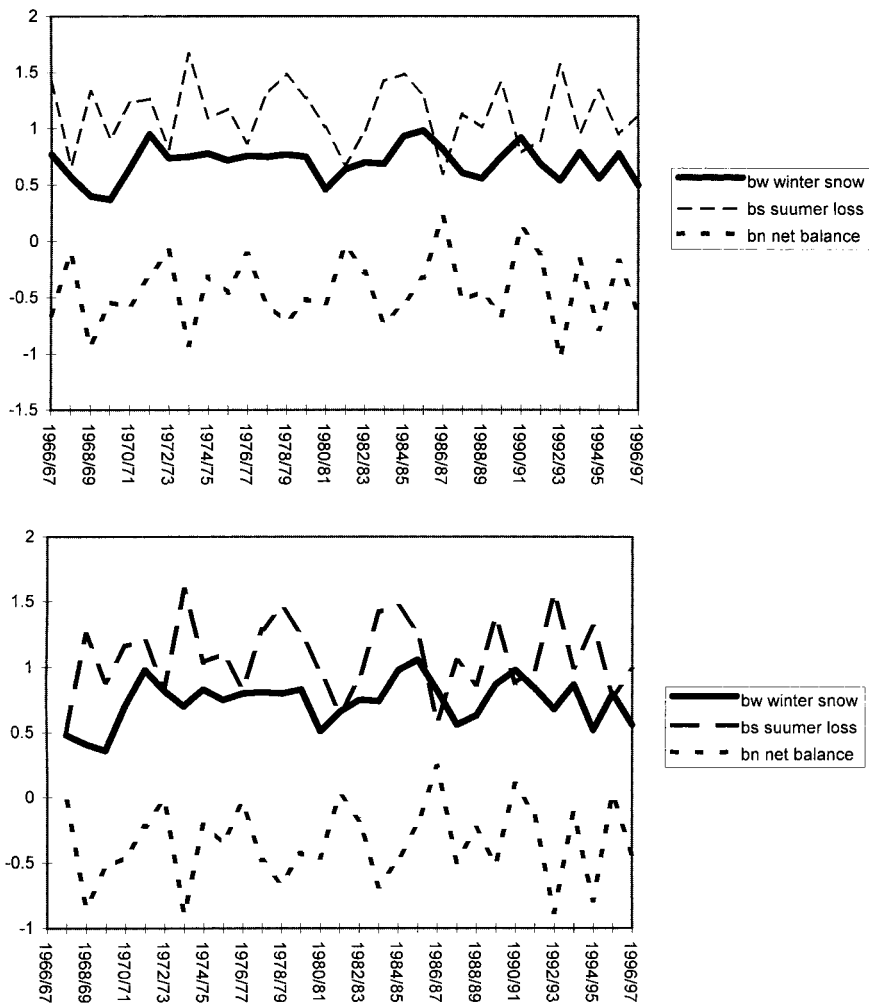


Figure 2. Winter, summer and net balances ( $B_w$ ,  $B_s$  and  $B_n$  respectively) for Austre Brøggerbreen (top) and Midre Lovénbreen (bottom) 1966/1967–1995/1996.  $B_s$  is shown with sign reversed

subtropical component is part of the subtropical ridge of the North Atlantic (Barnston and Livezey, 1987; Bell, 1998).

The East Atlantic Jet (EA JET) is a spring and summer mode of North Atlantic variability. This pattern, which displays considerable interdecadal variability, is of special interest to this study as the dipole which characterizes it has a locus of activity over the far eastern North Atlantic and Scandinavia. The subtropical component of the dipole is found near the Mediterranean Sea (Bell, 1998).

Eurasia is influenced by the East Atlantic/Western Russia (EA/WR) pattern (Barnston and Livezey, 1987) which in winter, has two main anomaly centres located over the Caspian Sea and western Europe. This simple pattern is replaced by a more complicated structure in spring and autumn, so that two main anomaly centres, of opposite sign, are found over western or northwestern Russia and over northwestern Europe. The third centre, (in phase with the Russia centre), is located off the Portuguese coast in spring, but moves westward in autumn (Bell, 1998).

Of immediate interest to this study is the main mode of variability over Scandinavia, Siberia and the Arctic Ocean known as the Scandinavia pattern (SCA) which is active in all months except the high summer (Barnston and Livezey, 1987). Blocking events over Scandinavia and Russia are objectively measured by this mode (Bell, 1998).

The West Pacific (WP) pattern is a primary mode of low-frequency variability over the North Pacific in all months (Barnston and Livezey, 1987; Wallace and Gutzler, 1981). During winter and spring, the pattern consists of a north-south dipole of anomalies, with an east-west Pacific band (including southeastern Asia and the subtropical latitudes of the far western North Pacific) opposing a centre located over the Kamchatka Peninsula. Zonal and meridional variations in the location and intensity of the entrance region of the Pacific (or East Asian) jet stream are therefore reflected in this mode (Wallace and Gutzler, 1981; Barnston and Livezey, 1987). Seasonal variability of this pattern is marked. In the summer and autumn, a third centre appears over Alaska and the Beaufort Sea, with a sign opposite to the centre over the western North Pacific (Bell, 1998).

The North Pacific (NP) pattern appears mostly in spring and summer, consisting of a main anomaly centre spanning the western and central North Pacific, and a smaller centre of opposite sign across eastern Siberia, Alaska and central North America. This mode is associated with a latitudinal shift in the Pacific jet stream between eastern Asia and eastern North Pacific (Bell, 1998).

The Pacific North American (PNA) pattern is perhaps the best known mode of Pacific based variability. It appears in all months except June and July. The PNA pattern reflects a quadrupole pattern of geopotential anomalies, with anomalies of similar sign located south of the Aleutian Islands and over the southeastern USA. Anomalies with sign opposite to the Aleutian centre are located near Hawaii, and over central Canada during the winter and autumn (Barnston and Livezey, 1987; Bell, 1998).

The PNA pattern is at its largest extent during winter, corresponding to the expanse of the Aleutian component of the mode across much of the North Pacific. The pattern undergoes major seasonal changes such that in spring, the subtropical centre covers a very large part of the Pacific but the Aleutian centre becomes confined to the Gulf of Alaska. The pattern is not identifiable during June and July and is confined mainly to the landmass and the North Pacific during spring. This modulation appears to link the PNA pattern directly with Rossby wavetrains associated with the seasonal modulation of the strength of the zonal westerlies (Barnston and Livezey, 1987).

The Tropical Northern Hemisphere (TNH) pattern (Mo and Livezey, 1986; Barnston and Livezey, 1987) consists of one primary anomaly centre over the Gulf of Alaska and a separate anomaly centre of opposite sign over Hudson Bay. A weaker area of anomalies, having similar sign to the Gulf of Alaska anomaly, extends across Mexico and the extreme southeastern USA. Taken together, these centres indicate large-scale changes in both the location and eastward extent of the Pacific jet stream.

The procedure used initially to identify the teleconnection patterns discussed in this section is outlined in detail in Barnston and Livezey (1987). They used Rotated Principal Component Analysis (RPCA) to isolate the primary teleconnection patterns in the Northern Hemisphere circulation for all months. Here the results from an RPCA technique applied to monthly mean 700-mb height anomalies between January 1964 and July 1994 are used (Bell and Halpert, 1995; Bell, 1998). The indices are the time coefficients (or amplitudes) of the RPCA modes which have been calculated over the standard seasons December–February (DJF), March–May (MAM), etc. Indices reflecting the amplitudes of all the patterns discussed in Section 3 have been used in this study (Table I). Where a mode of variability only occurred for part of the standard seasons defined above, only those available months were used.

#### 4. STATISTICAL METHODS

Both Pearson and Spearman's rank correlation techniques have been used in this analysis to determine the standardized covariance between parameters of glacial mass balance and the amplitudes of Northern Hemisphere modes of variability for the period 1966–1996. Since no transformation has been applied to the data, Pearson correlation coefficients have been calculated for variables that are normally distributed but Spearman's rank correlation has been used for those that failed a simple test for normality. While Ramage (1983), amongst others, has alluded to the hazards of using correlation as a climatological tool, it remains an extensively used and simple method.

Table I. Northern Hemisphere Teleconnection patterns (and abbreviations) used in this study (based on Barnston and Livezey, 1987 and Bell, 1998)

Abbreviation	Name
NAO	North Atlantic Oscillation
EA	East Atlantic
EA JET	East Atlantic Jet
EA/WR	East Atlantic/Western Russia
SCA	Scandinavia
WP	West Pacific
EP	East Pacific
NP	North Pacific
PNA	Pacific North American
TNH	Tropical Northern Hemisphere

Lagged and lead correlations have been extensively considered in this study. Such correlations may be stronger than simultaneous relationships and provide insight into the physical mechanisms operating in these associations. If sufficiently strong, they also suggest scope for forecasting. Both lag and lead correlations have therefore been calculated. Estimates of significance are based on the t-test, but include adjustments for reduced degrees of freedom resulting from autocorrelation.

Principal components have been used to reduce the dimensionality of the mass balance data sets. This technique has been widely used in climatology and meteorology for this purpose (see Joliffe, 1986 for a full discussion of principal components). The time coefficients (or scores) of the principal components are used as new mass balance indices that best summarize historical conditions on the two glaciers considered.

## 5. MASS BALANCE INDICES

We start with the interpretation of the glacial mass balance data. Since our aim is to correlate indices of glacial mass balance with global sea level pressure at lag, lead and simultaneous seasonal time scales, an *a priori* selection of the mass balance indices is necessary in order to reduce the total potential number of correlation coefficients.

Figure 3 shows the spectral estimates of the individual mass balance parameters at each of the glaciers. Significant spectral power (5% level using a chi-squared test) is concentrated near 7 years in the case of winter snow accumulation, but has two significant peaks (4.6 and 2.3) for the remaining eight indices (i.e.  $B_s$ ,  $B_n$ , AAR, ELA on each glacier). There is good agreement between the spectral decomposition parameters on each glacier, although the spectral peak in the case of  $B_w$  is larger for Midre Lovénbreen.

Redundancy in the glacial mass balance indices is also indicated by the high modulus of correlation values in the glacial index correlation matrix (not shown). This has been noted as a general characteristic of such indices (Lindeman and Oerlemans, 1987) and results, in part, from the definition of these indices. Correlations between indices such as net balance versus ELA may be less pronounced, since this relationship may be a function of factors such as glacial geometry. Rather than arbitrarily selecting certain indices, principal components of the ten indices have been calculated in order to reduce the dimensionality of the data set, whilst retaining the shared variance and hence the signal expressed by the collective mass balance indices (Joliffe, 1986).

Principal Components (PCs) of the ten mass balance indices ( $B_w$ ,  $B_s$ ,  $B_n$ , ELA, AAR for each of the glaciers) have been calculated using the indices as variables and the years as observations (P and S mode decomposition). The first two PCs account for 96.5% of the variance, with the first PC capturing 75% of the total variance (Table II). The correlation form of the eigenvectors is shown in Table III. PC1 loads highly on all indices except for  $B_w$  on either glacier. This is accounted for in PC2. That  $B_s$  and  $B_w$  should load on different PCs is clear from contrasting spectral decomposition of these indices. This division is also consistent with other work which treat  $B_w$  and  $B_s$  separately (Holmlund, 1987; Pohjola and Rogers, 1997b).

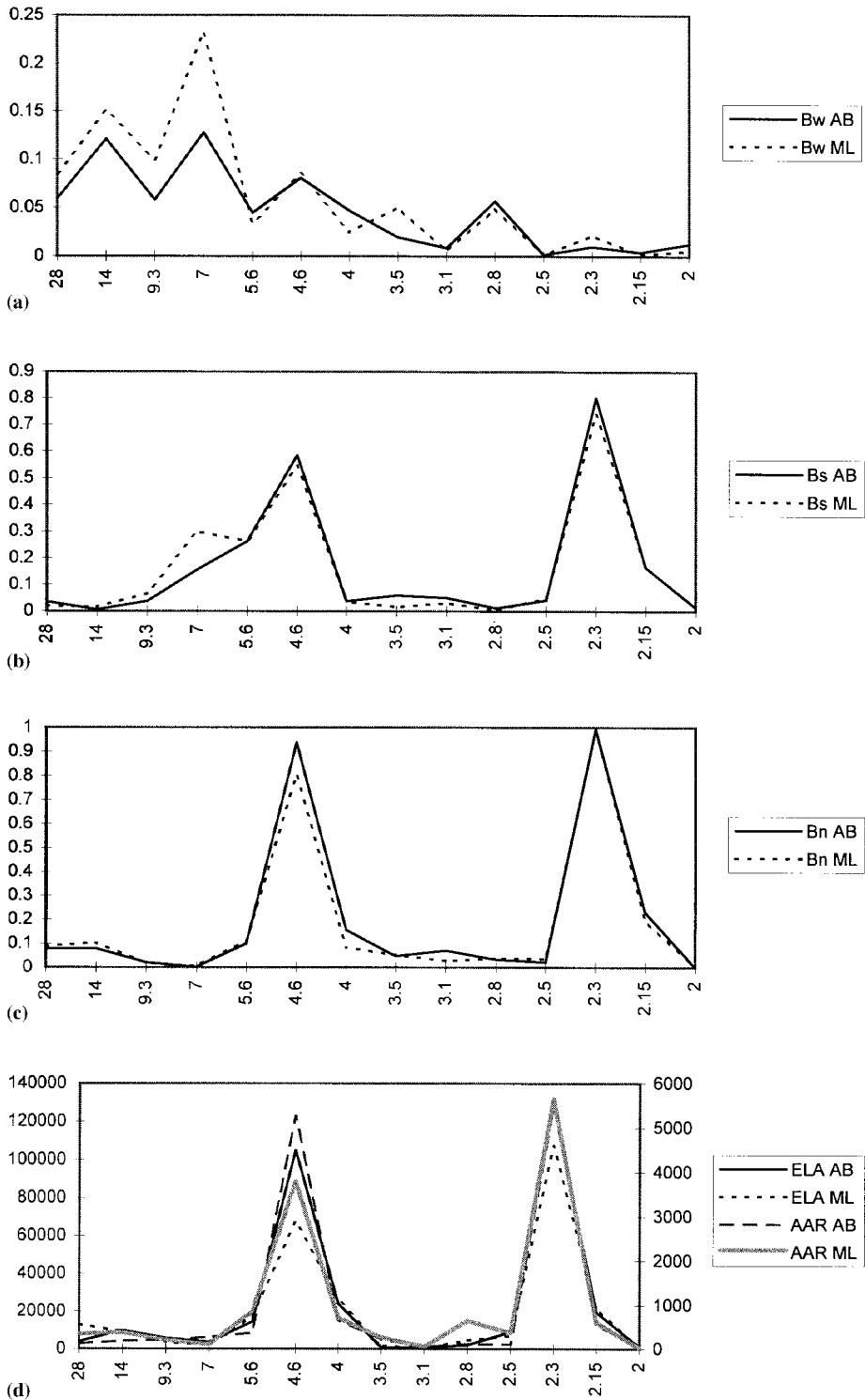


Figure 3. Spectra of  $B_w$  (a),  $B_s$  (b),  $B_n$  (c), ELA and AAR (d) for Midre Lovénbreen and Austre Brøggerbreen (ML and AB, respectively). Period (horizontal axis) is plotted against the periodogram ordinates (vertical axis)

Table II. Eigenvalues and associated variance of PC1 and PC2

	PC1	PC2
Eigenvalue	7.4686	2.1765
Difference	5.2921	2.0495
Proportion	0.7469	0.2177
Cumulative	0.7469	0.9645

The time coefficients (product of the eigenvectors and the standardized mass balance indices) of PC1 and PC2 have been calculated to create new indices of mass balance, with PC1 expressing mass balance factors associated with summer melt and PC2 the winter snow accumulation. These new indices (here called PC1 and PC2) were then correlated with the Northern Hemisphere teleconnection indices.

## 6. MASS BALANCE–ATMOSPHERIC CIRCULATION RELATIONSHIPS

Correlations between each of these PC time coefficients and the teleconnection indices discussed in Section 3 are shown in Tables IV and V. Significant correlations (95% level) are shown for simultaneous seasons (i.e. of the same calendar year) as well as lead seasons (e.g. SON (September–November) – 1 atmospheric index leads the mass balance index) and lag (e.g. MAM + 1 atmospheric index lags the mass balance index) up to one calendar year either side of the mass balance year.

PC1 (summer melt component of mass balance) has the highest correlation with the spring index of the EA JET pattern ( $r = 0.51$ ). At leads of one and two seasons (DJ and November, respectively), the phase and strength of the TNH pattern is the most important association. The most frequently occurring lead signals emerge from the Pacific Ocean (TNH and WP). No significant correlations are found with summer teleconnection indices and the summer melt as expressed by PC1, although this partly reflects the reduced frequency of summer teleconnection patterns used in the study. Correlations with the TNH pattern show a sign change between the lead season (November  $r = 0.42$ ) and the simultaneous season DJ ( $r = -0.40$ ).

PC2, which is taken to represent variability of the combined winter accumulation component ( $B_w$ ) of each glacier, has the highest simultaneous correlation (DJF season) with the EA/WR pattern ( $r = 0.52$ ), but slightly stronger correlation at a one season lead with the PNA pattern ( $r = -0.54$ ). It is remarkable that signals from the Pacific appear to have a stronger association with mass balance components than modes of variability based in the Atlantic. As with the PC1 correlations, we find that the correlations between PC2 and the PNA pattern reverse sign depending on the lead (positive in DJF simultaneous, negative in SON – 1). Lag correlations are confined to the Atlantic sector, the highest of which is with the

Table III. Eigenvector weights of the mass balance indices

	PC1	PC2
Austre Brøggerbreen		
$B_w$	0.42228	0.89277
$B_s$	0.86484	0.48023
$B_n$	0.98635	0.01026
ELA	-0.98177	-0.03919
AAR	0.95930	-0.03952
Midre Lovénbreen		
$B_w$	0.37358	0.91250
$B_s$	0.82650	0.54975
$B_n$	0.98927	0.00739
ELA	-0.96443	-0.09335
AAR	0.97666	0.04484

Table IV. Significant correlations (95%) between summer melt (PC1) and Northern Hemisphere Teleconnection Indices for monthly or seasonal simultaneous, lag and lead times, 1966–1997

Season	Index	Correlation
Aug – 1	SCA	0.38
SON – 1	EA/WR	–0.38
Nov – 1	TNH	0.42
DJF	WP	0.30
DJ	TNH	–0.40
AM	EA JET	0.51
MAM	NP	–0.35
SON	EA	0.36
SON	WP	–0.35
MAM + 1	EA/WR	0.40
JJ + 1	NP	0.39

SON, September–October; DJF, December–January; DJ, December–January; AM, April–May; MAM, March–May; SON, September–November; JJ, June–July.

EA pattern ( $r = 0.51$ ). The most frequently occurring significant correlation is with the PNA pattern and the most frequently occurring lead signals originate from the Pacific sector.

Table VI shows the correlations between teleconnection indices and the individual mass balance components of the two glaciers separately, but only for cases where the modulus of the correlation exceeds that calculated for the PC based mass balance indices and where correlations are significant at the 95% level. Taken separately,  $B_w$  is related in part to the EA/WR pattern ( $r = 0.52$  and  $r = 0.54$  for Midre Lovénbreen and Austre Brøggerbreen, respectively), but, remarkably, the strongest correlation calculated in the course of this study emerges at a 1 year lead from the TNH for Midre Lovénbreen ( $r = 0.60$ ) with  $B_w$ . The correlation at the same lead with the TNH pattern for Austre Brøggerbreen is only slightly weaker ( $r = 0.58$ ). Simultaneous correlations for the winter high season are also higher for individual mass balance parameters than those for the PC indices, for example the correlation between  $B_w$  for Midre Lovénbreen and the NAO.

$B_s$ , on the other hand, is influenced moderately to strongly by the EA JET pattern (in AM,  $r = 0.57$ ) and weakly by the TNH ( $r = -0.39$ ) and EA/WR ( $r = -0.40$ ) pattern in the case of Austre Brøggerbreen (see Table VI). Correlations for the summer melt component for Midre Lovénbreen are close to those represented by the PC based indices discussed earlier (Tables IV and V).

Table VI shows that  $B_n$  has the strongest association with the EA JET pattern in AM for both glaciers. Both the TNH and PNA patterns are nevertheless important at lead times, although correlations with the TNH pattern change sign between seasons. In most cases the ELA and AAR indices are weakly correlated with teleconnection patterns with the Midre Lovénbreen based correlations being noticeably weaker than those for Austre Brøggerbreen (not shown). The weaker correlations for the ELA and AAR are unsurprising because both these indices were derived from the original mass balance parameters and are additionally influenced by the hypsometry of the glacier basins.

Table V. Significant correlations (95%) between winter accumulation (PC2) and Northern Hemisphere Teleconnection Indices for monthly or seasonal simultaneous, lag and lead times, 1966–1997

Season	Index	Correlation
SON – 1	PNA	–0.54
DJF	PNA	0.41
DJF	EA/WR	0.52
SON	NAO	0.34
AM + 1	EA JET	0.40
SON + 1	EA	0.51

Season abbreviations as in Table IV.

Table VI. Correlations between mass balance indices from individual glaciers and teleconnection indices<sup>a</sup>

Season	Index	Correlation
Austre Brøggerbreen		
DJ-1	$B_w$ -TNH	0.58
Aug-1	$B_s$ -PNA	0.42
Aug-1	$B_s$ -SCA	0.46
SON-1	$B_s$ -EA/WR	-0.40
Nov-1	$B_n$ -TNH	0.41
DJF	$B_w$ -EA/WR	0.54
DJ	$B_s$ -TNH	-0.39
DJ	$B_n$ -TNH	-0.42
AM	$B_s$ -EA JET	0.57
AM	$B_n$ -EA JET	0.59
DJ+1	$B_s$ -TNH	0.39
MAM+1	$B_s$ -EA/WR	0.45
Midre Lovénbreen		
DJ-1	$B_w$ -TNH	0.60
Aug-1	$B_s$ -PNA	0.46
Aug-1	$B_n$ -PNA	0.35
SON-1	$B_s$ -EA/WR	-0.44
DJF	$B_w$ -PNA	0.45
DJF	$B_w$ -EA/WR	0.52
MAM	$B_w$ -NAO	0.44
AM	$B_n$ -EA JET	0.53
SON	$B_s$ -WP	-0.40
AM+1	$B_s$ -EA/WR	0.57
JJ+1	$B_n$ -NP	0.43

Season abbreviations as in Table IV.

<sup>a</sup> Only cases where the modulus of the correlation exceeds that found for the PC based mass balance indices are listed (i.e. where the individual mass balance parameters on each glacier show a higher correlation compared with the combined parameters).

## 7. INTERPRETING NORTHERN HEMISPHERE MODES AND MASS BALANCE

Glacial mass balance reflects an important signal of climate variability and change. In much of the middle and high latitudes, the energy associated with the atmospheric component of the climate system is transferred through advection in standing and transient eddies (Grotjahn, 1993). The spatial pattern of time mean modes of variability associated with these eddies and hence energy advection, may be assessed in the form of eigenvectors of a representative variable such as 700 hPa heights. Equipped with a data set of the time wise amplitude of such modes, we may explore the degree of connectivity between patterns of hemispheric wide circulation and the multivariate record that glaciers provide. In doing so we are able to move beyond the confines of the microscale energy balance type studies, to the planetary organization of the atmosphere, at which scale important change and variability is orchestrated.

This study shows that distant modes of variability, originating sometimes as tropical thermal forcing in the ocean-atmosphere interface, but propagating as low wave number quasi-stationary Rossby waves in the midlatitudes, appear to have considerably more association with glacial mass balance variability than localized modes, whose signal might intuitively be thought to impose a higher amplitude thermal and mass forcing on the immediate glacial environment.

Modes which have strong association with the PC derived mass balance indices include the TNH and PNA. The PNA in particular, has the highest magnitude of any of the correlations. Correlations with the individual mass balance components similarly demonstrate the significance of the TNH pattern, which records the highest correlation found in this study (with  $B_w$  on Midre Lovénbreen).

The TNH signature is directly linked with the modulation of the Pacific jet stream which, in turn, determines the flow of marine air into North America and the southward transport of cold Canadian air into the north-central USA (Bell, 1998). TNH episodes have been associated with large El Niño–Southern Oscillation (ENSO) events such that a negative Southern Oscillation Index is associated with a negative TNH pattern (Barnston *et al.*, 1991). Why a positive/negative TNH pattern appears to enhance/suppress winter snow accumulation and net balance in Svalbard 1 year later is not immediately clear. To gain some insights, we correlated the TNH pattern amplitude with Northern Hemisphere sea level pressure so that the TNH amplitudes lead the sea level pressure data by 1 year (Figure 4). We used the Global Mean Sea Level Pressure data set (GMSLP21F) (Basnett and Parker, 1997) at a 5° latitude by 5° longitude for the years 1951–1994 over the DJF season. Although the correlations are weak to moderate, it is clear that 1 year after a positive/negative TNH episode, pressure is anomalously high/low in the northern subtropics

### TNH Vs GMSLP21 DJF -1

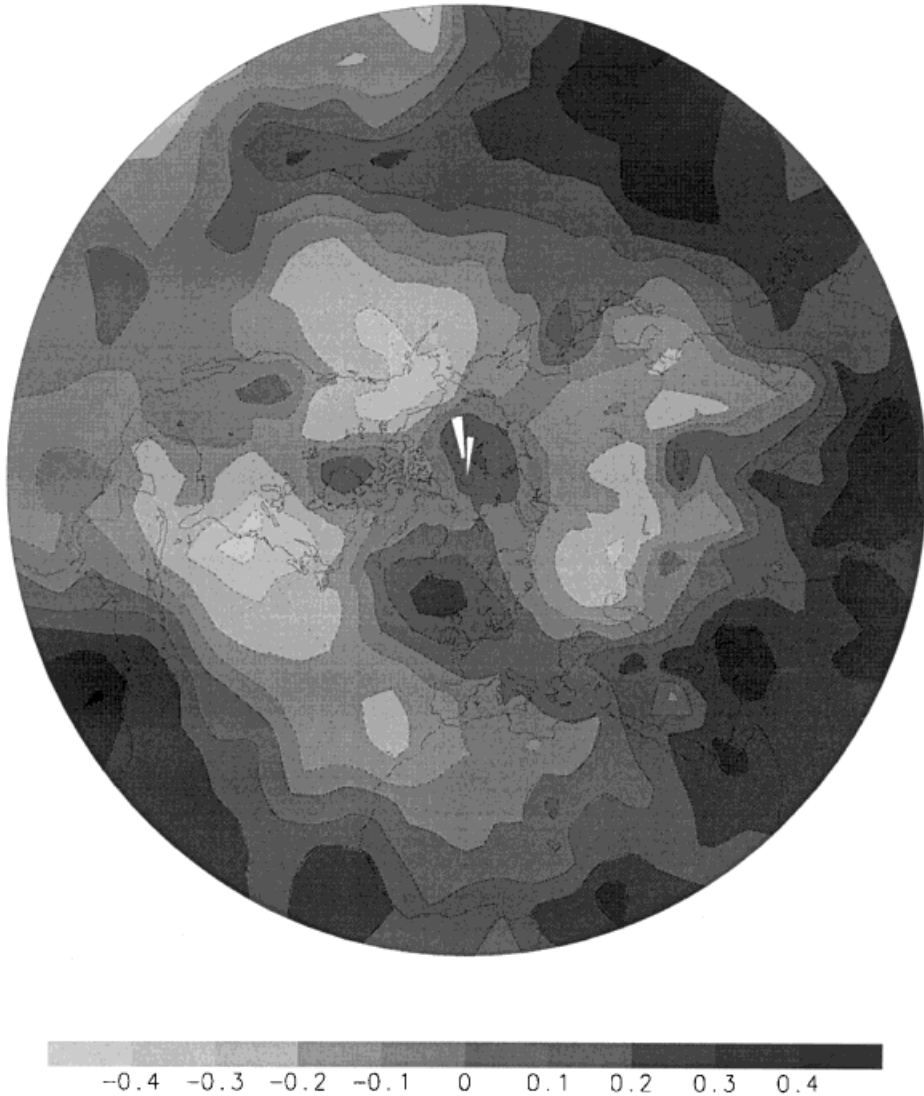


Figure 4. Correlations between TNH pattern amplitudes for DJF and DJF sea level pressure at 1 year lead (TNH index leading the sea level pressure) for 1951–1994

but anomalously low/high in the middle to polar latitudes. It follows that a strengthened/weakened geostrophic wind follows TNH positive/negative episodes, although the relationship is not strong. This is consistent with increased/decreased winter snow in Svalbard and perhaps for many other locations at this latitude.

The correlation between SON PNA pattern and PC2 (winter snow accumulation) similarly indicates an atmospheric response at delayed time scales to an essentially Pacific based feature. Correlations between SON PNA pattern amplitude and following DJF sea level pressure are shown in Figure 5 for the years 1951–1994. The correlations show a large scale Atlantic response such that a positive/negative PNA pattern is followed by anomalously high/low pressures in the North Atlantic but anomalously low/high pressures in the South Atlantic, consistent with the negative correlation between SON PNA amplitudes and PC2 which suggest reduced snow accumulation on Svalbard glaciers.

### PNA Vs GMSLP21 SON -1

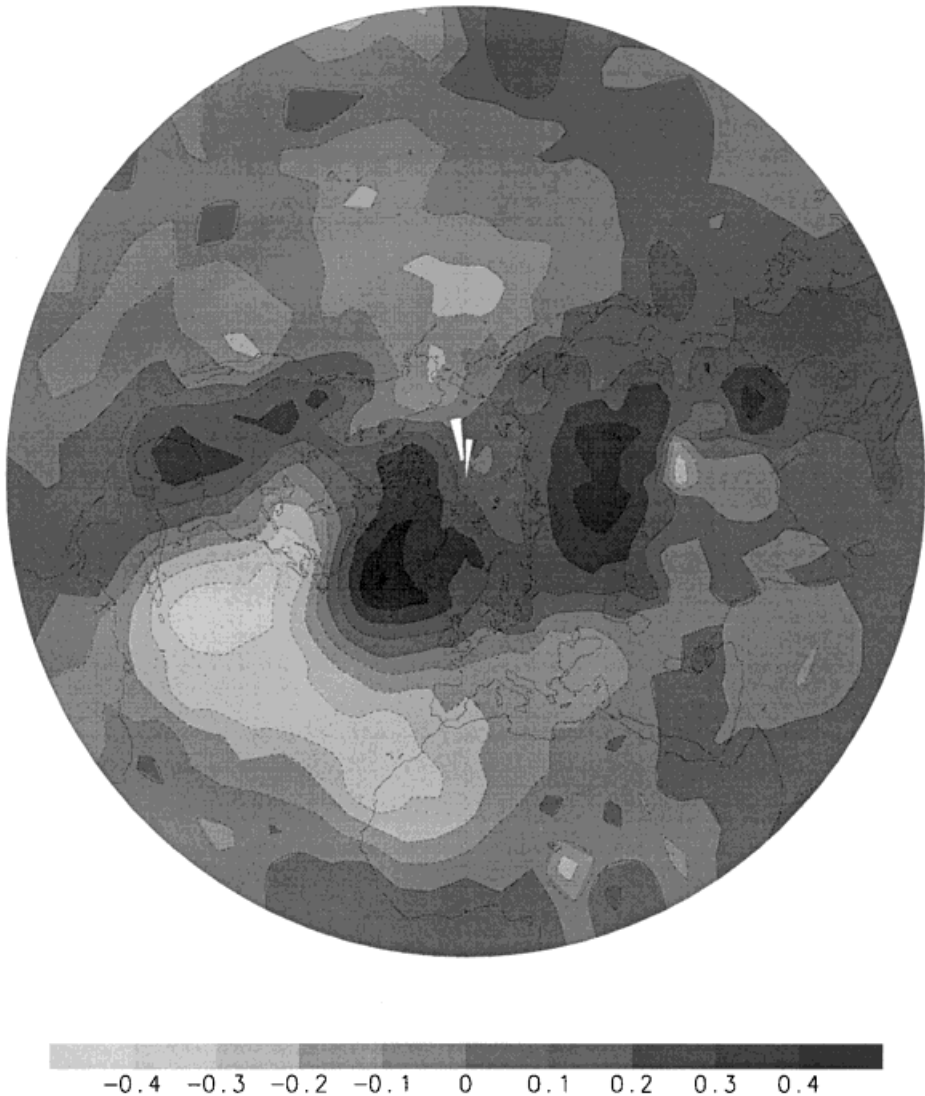


Figure 5. Correlations between PNA pattern amplitudes for SON and DJF sea level pressure at one season lead (PNA index leading the sea level pressure) for 1951–1994

While further investigation is beyond the scope of this paper, equally interesting relationships are likely to lie behind time lagged correlations with the NP and WP pattern. Instead of focussing on these, we turn to Atlantic based patterns which, not surprisingly, have high simultaneous correlations with both summer melt and winter accumulation related mass balance parameters (as expressed by PC1 and PC2). High/low summer melt is associated with the positive/negative phase of the EA JET pattern in spring. It is plausible that the intensification of westerlies associated with the positive phase of the EA JET pattern leads to an anomalously high transport of sensible heat in the transient eddies to the high latitudes in spring. Blocking during these months in the vicinity of Greenland, which is associated with the negative phase of this pattern, would lead to reduced heat flux and hence reduced summer melt.

That correlations between mass balance parameters and teleconnection indices reach a maximum at time leads of seasons to years, suggests predictability of glacial mass balance at intraseasonal to interannual time scales. The correlation between summer melt and AM EA JET ( $r = 0.57$ ) for Austre Brøggerbreen, is encouraging. Given that Northern Hemisphere modes of variability are characterized by pronounced decadal variability (e.g Hurrell, 1995), longer term predictability is also conceivable. The time series of the EA JET pattern, for example, exhibits considerable interdecadal variability. The 1971–1978 period was dominated by the negative phase of the pattern, while the 1985–1993 period was characterized by a positive phase in 70% of the seasons. Similarly, an increased frequency of ENSO warm phase episodes in the last three decades impacts on the phase of the PNA pattern.

A detail of this study is the reverse of the correlation sign between circulation mode indices and mass balance parameters on seasonal leads. For example, PC1 correlates positively with the TNH pattern amplitudes in the preceding November, but negatively during the DJ (simultaneous) season. This suggests that summer melt is sensitive to the timing of a TNH signal in seasons prior to the summer melt. Thus, both the longevity and genesis date of TNH events are also of relevance.

Given the prominence of the NAO as a mode of Northern Hemisphere variability (Barnston and Livezey, 1987), the lack of significant or large correlations between mass balance indices and this mode is remarkable. Likewise, the SCA pattern appears to have limited influence. The modes derived originally by Barnston and Livezey (1987) represent the main patterns of Northern Hemisphere variability well, but are not necessarily the modes of variability in the atmosphere which are optimally coupled with glacial mass balance in the High Arctic. Other methods would be necessary to identify these. Furthermore, no single teleconnection index appears to explain the variance in the mass balance indices, instead several patterns appear to have an influence. Scope therefore exists to model the behaviour of the mass balance indices through a combination of the teleconnection indices.

## 8. CONCLUSIONS

The aim of this paper was to determine the relationship between the amplitudes of patterns of Northern Hemisphere circulation variability and mass balance indices for two glaciers in Svalbard. It emerges that several distant teleconnections to Svalbard glacial mass balance exist. Indeed, the strongest correlations are found with Pacific based patterns such as the PNA and TNH, suggesting that tropical signals may impact on glacial ablation and advance within a year of emerging from the tropical Pacific as anomalous heat fluxes. The timing of these relationships also suggests that glacial conditions may be predictable on intraseasonal to interdecadal time scales. There is, however, much that can be done to refine these relationships.

## ACKNOWLEDGEMENTS

RW would like to thank the University of Oxford for funding computing resources. Jon Ové Hagen and Bernard Lefauconnier are thanked for their comments on an earlier version of this manuscript. Thanks also to Brad Delp and Tom Scholz.

## REFERENCES

- Barnston AG, Livezey RE. 1987. Classification, seasonality and persistence of low-frequency atmospheric circulation patterns. *Monthly Weather Review*. **115**: 1083–1126.
- Barnston AG, Livezey RE, Halpert MS. 1991. Modulation of Southern Oscillation–Northern Hemisphere mid-winter climate relationships by the QBO. *Journal of Climate*. **4**: 203–217.
- Basnett TA, Parker DE. 1997. *Development of the Global Mean Sea Level Pressure Data Set GMSLP2*, Report to DoE, Hadley Centre, Meteorological Office, Bracknell, UK.
- Bell GD, Halpert MS. 1995. *Atlas of Intraseasonal and Interannual Variability, 1986–1993*. NOAA Atlas No. 12. Climate Prediction Center, NOAA/NWS/NMC: Washington.
- Bell GD. 1998. <http://nic.fb4.noaa.gov/data/teledoc/telecontents.html>
- Esbensen SK. 1984. A comparison of intermonthly and interannual teleconnections in the 700 mb geopotential field during the Northern Hemisphere winter. *Monthly Weather Review*. **112**: 2016–2032.
- Fitzharris BB, Hay JE, Jones PD. 1992. Behaviour of New Zealand glaciers and atmospheric circulation changes over the past 130 years. *Holocene*. **2**(2): 97–106.
- Fleming KM, Dowdeswell JA. 1997. Modelling the mass balance of northwest Spitsbergen glaciers to climate change. *Annals of Glaciology*. **24**: 203–210.
- Gloersen P. 1995. Modulation of hemispheric sea-ice cover by ENSO events. *Nature*. **373**: 503–506.
- Grotjahn R. 1993. *Global Atmospheric Circulations*. Oxford University Press: New York.
- Haerberli W. 1995. Glacier fluctuations and climate change detection—operational elements of a worldwide monitoring strategy. *Bulletin of the World Meteorological Organisation*. **44**: 23–31.
- Haerberli W, Hoelzle M. 1995. Application of inventory data for estimating characteristics of and regional climate change effects on mountain glaciers—a pilot study with the European Alps. *Annals of Glaciology*. **21**: 206–212.
- Hagen JO, Liestøl O. 1990. Long term glacier mass balance investigations in Svalbard, 1950–88. *Annals of Glaciology*. **14**: 102–106.
- Hagen JO, Sætang A. 1991. Radio-echo soundings of sub-polar glaciers with low frequency radar. *Polar Research*. **9**: 99–107.
- Hastenrath S, Kruss PD. 1988. The role of radiation geometry in the climate response of Mount Kenya's glaciers, part 2: sloping versus horizontal surfaces. *International Journal of Climatology*. **8**: 629–639.
- Hay JE, Fitzharris BB. 1988. The synoptic climatology of ablation on a New Zealand glacier. *Journal of Climatology*. **8**: 201–215.
- Hodson AJ, Gurnell AM, Washington R, Clark MJ, Tranter M. 1998. Meteorological and runoff time series from a High-Arctic, glaciated basin, Svalbard. *Hydrological Proceedings*. **12**(3): 509–526.
- Horel JD. 1981. A rotated principal component analysis of the interannual variability of the Northern Hemisphere 500 mb height field. *Monthly Weather Review*. **109**: 2080–2092.
- Holmlund P. 1987. Mass balance of Storglaciären during the 20th century. *Geographical Annals*. **69A**: 439–447.
- Hurrell JW. 1995. Decadal trends in the North Atlantic Oscillation: regional temperatures and precipitation. *Science*. **269**: 676–679.
- Hurrell JW. 1996. Influence of variations in extratropical wintertime teleconnections on Northern Hemisphere temperature. *Geophysical Research Letters*. **23**(6): 665–668.
- Ishikawa N, Owens IF, Sturman AP. 1992. Heat balance characteristics during fine periods on the lower parts of Franz Josef glacier, South Westland, New Zealand. *International Journal of Climatology*. **12**: 397–410.
- Jolliffe IT. 1986. *Principal Component Analysis*. Springer-Verlag: Berlin.
- Lefauconnier B, Hagen JO. 1990. Glaciers and climate in Svalbard: statistical analysis and reconstruction of the Brøggerbreen mass balance for the last 77 years. *Annals of Glaciology*. **14**: 148–152.
- Lindeman M, Oerlemans J. 1987. Northern hemisphere ice sheets and planetary waves: a strong feedback mechanism. *International Journal of Climatology*. **7**: 109–117.
- Mo KC, Livezey RE. 1986. Tropical–extratropical geopotential height teleconnections during the Northern Hemisphere winter. *Monthly Weather Review*. **114**: 2488–2515.
- Mote TL. 1998. Mid-tropospheric circulation and surface melt on the Greenland ice sheet. Part 1: atmospheric teleconnections. *International Journal of Climatology*. **18**: 111–130.
- Pohjola VA, Rogers J. 1997a. Coupling between the atmospheric circulation and extremes of mass balance of Storglaciären, northern Scandinavia. *Annals of Glaciology*. **24**: 229–233.
- Pohjola VA, Rogers J. 1997b. Atmospheric circulation and variations in Scandinavian Glacier Mass Balance. *Quaternary Research*. **47**: 29–36.
- Ramage CS. 1983. Teleconnections and the seige of time. *Journal of Climatology*. **3**: 223–231.
- Repp K. 1988. The hydrology of Bayelva, Spitsbergen. *Nordic Hydrology*. **19**: 259–268.
- Rogers JC, Van Loon H. 1979. The seesaw in winter temperatures between Greenland and northern Europe. Part II: Some ocean and atmospheric effects in middle and high latitudes. *Monthly Weather Review*. **107**: 509–519.
- Tyson PD, Sturman AP, Fitzharris BB, Mason SJ, Owens IF. 1997. Circulation changes and teleconnections between glacial advances on the west coast of New Zealand and extended spells of drought years in South Africa. *International Journal of Climatology*. **17**(14): 1499–1512.
- van Loon H, Rogers JC. 1978. The seesaw in winter temperatures between Greenland and northern Europe. 1. General description. *Monthly Weather Review*. **106**: 296–310.
- Walker GT. 1924. Correlation in seasonal variations of weather, IX. A further study of world weather. *Memoirs of the India Meteorological Department*. **24** (Part IV): 75–131.
- Walker GT, Bliss EW. 1932. World weather V. *Memoirs of the Royal Meteorological Society*. **4**: 53–84.
- Wallace JM, Gutzler DS. 1981. Teleconnections in the geopotential height field during the Northern Hemisphere winter. *Monthly Weather Review*. **109**: 784–812.
- Warrick RA, Le Provost C, Meier MF, Oerlemans J, Woodworth PL. 1996. Changes in sea level. In *Climate change 1995: The Science of Climate Change*, Houghton JT (ed.). Cambridge University Press.

- Yarnal B. 1984a. Synoptic-scale atmospheric circulation over British Columbia in relation to the mass balance of Sentinel glacier. *Annals of the Association of American Geographers*. **74**: 374–392
- Yarnal B. 1984b. Relationships between synoptic-scale atmospheric circulation and glacier mass balance in south-western Canada during the International Hydrological Decade, 1965–1974. *Journal of Glaciology*. **30**: 188–198.